Takashi Oishi
and
Susumu Tachi
RCAST
The University of Tokyo
4-6-1 Komaba, Meguro-ku
Tokyo, 153, Japan

Methods to Calibrate Projection Transformation Parameters for See-Through Head-Mounted Displays

Abstract

See-through head-mounted displays (STHMDs), which superimpose the virtual environment generated by computer graphics (CG) on the real world, are expected to be able to vividly display various simulations and designs by using both the real environment and the virtual environment around us. However, we must ensure that the virtual environment is superimposed exactly on the real environment because both environments are visible. Disagreement in matching locations and size between real and virtual objects is likely to occur between the world coordinates of the real environment where the STHMD user actually exists and those of the virtual environment described as parameters of CG. This disagreement directly causes displacement of locations where virtual objects are superimposed. The STHMD must be calibrated so that the virtual environment is superimposed properly. Among the causes of such errors, we focus both on systematic errors of projection transformation parameters caused in manufacturing and differences between actual and supposed location of user's eye on STHMD when in use, and propose a calibration method to eliminate these effects. In the calibration method, the virtual cursor drawn in the virtual environment is directly fitted onto targets in the real environment. Based on the result of fitting, the least-squares method identifies values of the parameters that minimize differences between locations of the virtual cursor in the virtual environment and targets in the real environment. After we describe the calibration methods, we also report the result of this application to the STHMD that we have made. The result is accurate enough to prove the effectiveness of the calibration methods.

1 Introduction

See-through head-mounted displays (STHMDs), which superimpose the virtual environment generated by computer graphics (CG) on the real world, can vividly display various simulations and designs by using the real environment around us. Such displays should simplify various tasks and improve performance efficiency because they graphically present information necessary to perform the task in three dimensions instead of document form.

However, information on the virtual environment or virtual objects must match the real environment because both environments are visible. This is one of the problems to be solved for practical use. Disagreement in matching locations and sizes between real and virtual objects is likely to occur between the world coordinates of the real environment where the STHMD user actually

Presence, *Vol. 5, No. 1, Winter 1996,* 122–135

exists and those of the virtual environment described as parameters of CG. Such disagreement directly causes displacement of locations where virtual objects are superimposed. The STHMD must thus be calibrated so that the virtual environment is superimposed properly.

The primary causes of such locational mismatch are

- distortion in the STHMD optical system,
- mechanical misalignments in the STHMD,
- differences between actual and designed location of user's eye,
- errors in the head-tracking system, and
- end-to-end system latency.

Several authors have discussed methods to eliminate such errors (Hirose, Kijima, Sato, & Ishii, 1990; Robinett & Rolland, 1992; McKenna & Zeltzer, 1992; Ma, Hollerbach, & Hunter, 1993; Janin, Mizell, & Caudell, 1993; Azuma & Bishop, 1994). In this paper, we will discuss the following two factors:

- mechanical misalignments in STHMD and
- differences between actual and designed location of user's eye.

We assume that there is no distortion in the optical system and that we have only to cope with the linear problems.

These two factors have both common and specific characteristics. The common characteristics are as follows:

- The virtual environment must be directly fitted onto the real environment point by point to ensure the matching of location and size between objects in both environments.
- These factors require only the modification of projection transformation. Hence we have to consider only how they change parameters.

The specific characteristics are that mechanical misalignments are eliminated by calibrating just once after STHMD fabrication, but eye position errors must be calibrated during initialization whenever STHMD is used. Hence, the STHMD may be fixed at a certain place in the real environment when we calibrate the mechanical misalignments. In contrast, the process of calibrating the users' viewpoint must be as easy for users as possible.

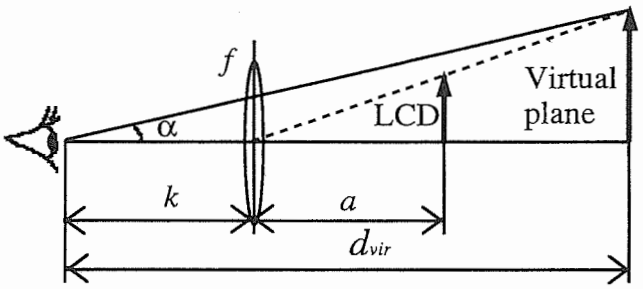

Figure 1. *Optical system of HMD.*

Based on these characteristics, we will propose a calibration method in which the virtual cursor projected by the STHMD was directly fitted onto targets in the real environment. We will also report the result of applying the method to the STHMD that we have made.

2 System Configuration

2.1 Designing and Manufacturing a Prototype of STHMD

An STHMD generates two virtual planes from planar images displayed on LCDs, one for the right eye and the other for the left. These images are placed at distance d_{vir}, which is derived from the optical system in Figure 1 as follows (Tachi & Arai, 1989):

$$d_{\text{vir}} = k + \frac{fa}{f - a} \tag{1}$$

The STHMD reproduces the binocular vergence and parallax, which are important for three-dimensional space perception, by projecting two images with the effect of parallax due to the interocular distance set during STHMD design. An image obtained at a viewpoint equivalent to the location of the left eye in the real environment is projected on the left virtual plane, and likewise for the right virtual plane.

The focus of the crystalline lens for the human operator is generally fixed at the distance d_{vir} to simplify the optical system as shown in Figure 1. Although the focus is not completely independent of the convergence due to the interaction, research is being conducted on the allowable disaccord between them. For example, it is

Table 1. *HMD Specifications*

Field of view			Interocular
Horizontal	Vertical	d_{vir}	distance
40°	30°	1 m	65 mm

known that the natural perception of three-dimensional (3D) space is possible for distances between 20 cm and infinity when d_{vir} = 1 m (Tachi & Arai, 1989). Hence, this becomes standard values of d_{vir} when designing the STHMD optical system.

Two 5.7-in. LCDs are used in our prototype. The wider the field of view, the better perception of 3D space. There is, however, a tradeoff because the image resolution decreases as the field of view increases. For example, see the specifications of our prototype shown in Table 1.

Figure 2 shows a portion of an STHMD containing optical systems. The eye mark roughly indicates the designed user eye locations. This portion is mounted on a full-face helmet so that the user can wear this optical system just in front of his or her face. "P" drawn in Figure 2b indicates a plate with marks used to calibrate the eye displacement. This will be described in Section 3.2. We shall also take this plate as the basis on which the dimensions of STHMD are defined. When we use expressions such as "designed location of the virtual plane" or "designed location of user's eye," we mean that they are measured from this plate and their values are given by the design.

2.2 Generating the Virtual Environment

To generate a virtual environment, we first define a "world coordinate system" in the CG program, then place the virtual objects relative to it. The projection transformation on this environment produces planar images, and these are projected on the LCDs (Fig. 3a).

Consider a point $\mathbf{V}$ whose cartesian components are V_X, V_Y, and V_Z in the environment. Its location expressed in the coordinate system W is $\mathbf{V}_W$. If we define a 4×4 homogeneous transform matrix T_{EW} that transforms a vector expressed in the coordinate system W to one expressed in the coordinate system E, i.e., $\mathbf{V}_E = T_{EW}\mathbf{V}_W$, the image of $\mathbf{V}$ projected on the plane is calculated as

$$\mathbf{V}_P = T_{PE_v}T_{E_vW_v}\mathbf{V}_{W_v} \tag{2}$$

Next, consider a point V′ in the real environment (Fig. 3b). Its location expressed in the coordinate system of the virtual plane is

$$\mathbf{V}'_V = T_{VE_r}T_{E_rS}T_{SW_r}\mathbf{V}'_{W_r} \tag{3}$$

The virtual environment, which we can see through the STHMD, simultaneously exists in the real environment. We can define W_v so that it correctly overlaps W_r, and since $\mathbf{V}'_{W_r}$ is known, we can also define $\mathbf{V}_{W_v}$ so that it satisfies

$$\mathbf{V}'_{W_r} = \mathbf{V}'_{W_v} = \mathbf{V}_{W_v} = \mathbf{V}_{W_r} \tag{4}$$

To superimpose the virtual environment precisely on the real one (i.e., $\mathbf{V}_P$, $\mathbf{V}'_V$ and the view point are on a straight line), it is necessary that $T_{E_vW_v} = T_{E_rS}T_{SW_r}$ and that T_{PE_v} is defined so that the projection plane correctly overlaps the virtual plane as shown in Figure 3c.

The realized location of the virtual plane is, however, likely to differ from designed location, i.e., T_{VE_r} may contain some error, and the error is unpredictable. Besides, the actual locations of the user's eyes, i.e., T_{E_rS}, are fixed only when the user wears the HMD (we assume that there is no error in T_{SW_r} in this paper). Therefore it is impossible to reflect these factors on T_{E_rS} beforehand.

The former problem is described in Section 3.1, and the latter in Section 3.2. Projection transformation parameters are viewpoint, line of sight, and shape of the projection plane (top, left), (bottom, right) at a certain distance l (Fig. 3a). Errors in T_{VE_r} are eliminated by modifying the line of sight and shape of the projection plane. To eliminate errors in T_{E_rS}, we have to modify the viewpoint and recalculate the other parameters based on it.

3 Calibrating to Eliminate Errors

3.1 Calibrating Mechanical Misalignments

Mechanical misalignments produce errors in the realized optical system of the HMD. As mentioned

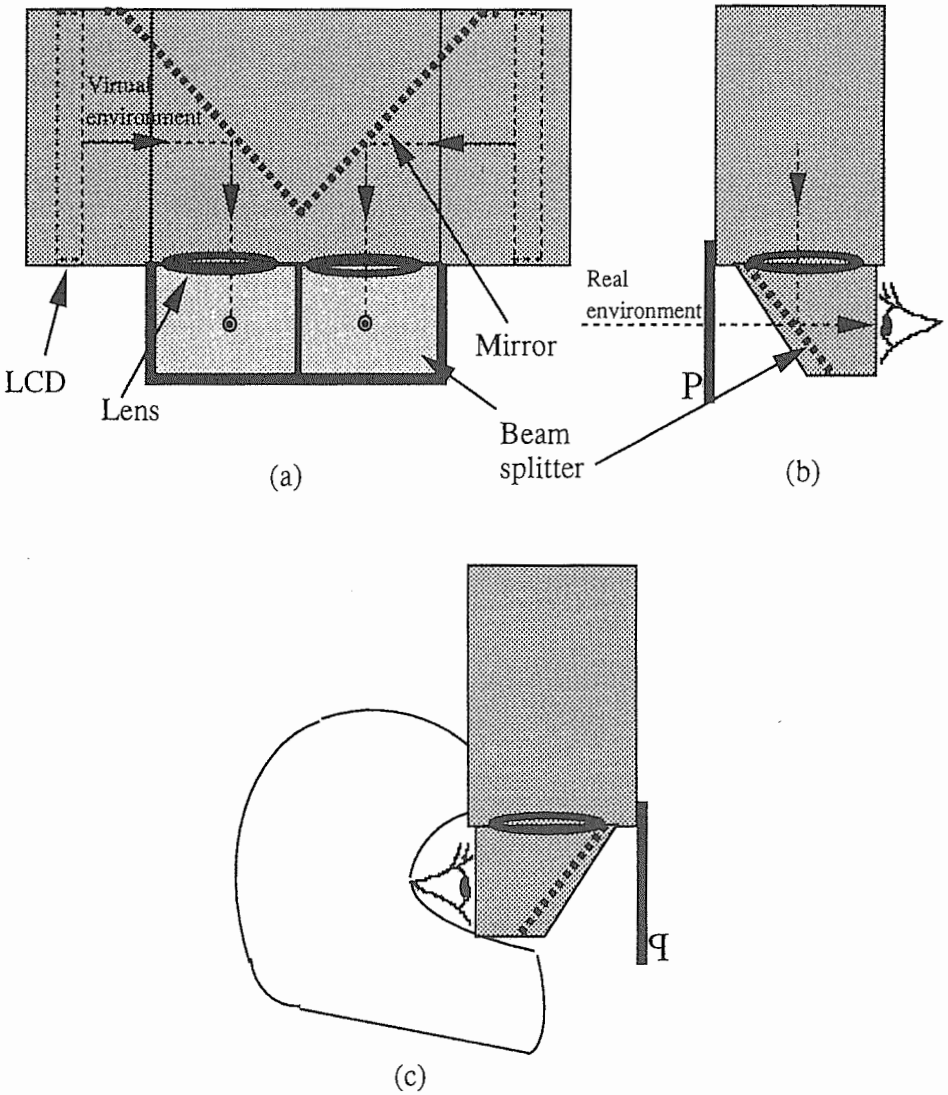

Figure 2. *Outline of HMD: (a) front view, (b) side view, (c) total setup.*

above, this is observed as the shift of virtual planes from the designed location. Figure 4 illustrates this shift.

A point a drawn in the virtual environment is projected onto the virtual planes for right and left eyes according to the designed locations of virtual planes. The projections for left and right eyes are designated as a_l and a_r. When the realized virtual plane for the right eye is not located as designed and is not reflected on the projection transformation parameters, a human operator detects the point at a'' instead of a, i.e., the location of a''_r on the realized virtual plane remains exactly the same as the location of a_r on the designed virtual plane. If the projection transformation parameters are set according to the realized location of the virtual plane, the image of point a is seen as a'_r. We must therefore measure the realized locations of virtual planes and modify the projection transformation parameters accordingly.

Figure 5 shows the calibration process. Here we describe each process.

3.1.1 Set HMD at the Origin of the World Coordinate of the Real Environment. The world coordinate system and marks for fitting are required in the real environment to measure the shift of the virtual plane

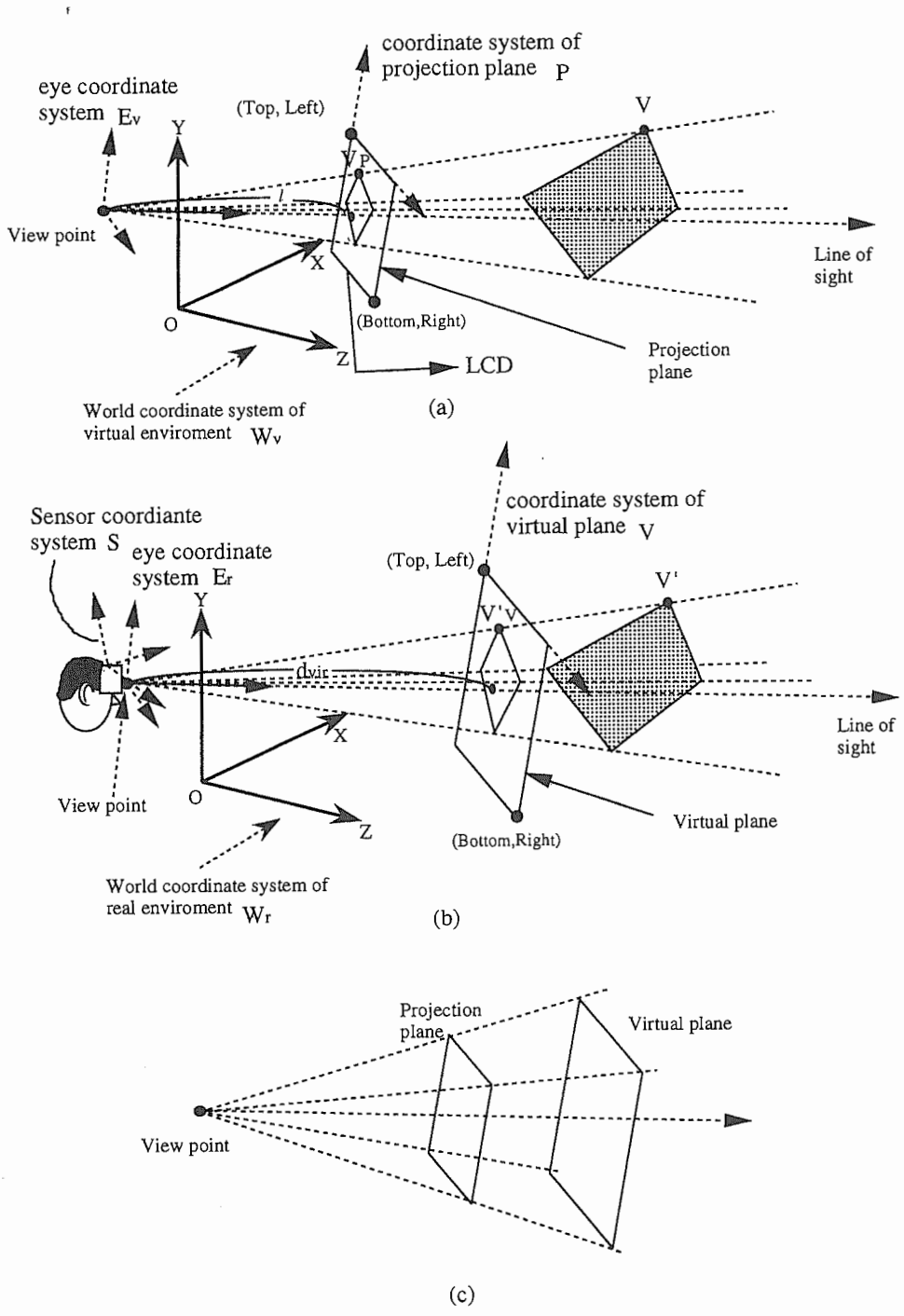

Figure 3. *Generation of virtual environment: (a) situation in the virtual environment, (b) the real environment, (c) locational relation desired between projection plane and virtual plane.*

and to perform the calibration. Figure 6 shows the measurement system used for calibration. LEDs marking position in the real environment are installed on the panel. The *Z* axis of the coordinate system runs through the panel's center and is perpendicular to it. The Y axis is a vertical line, and the *X* axis is assigned to constitute a right-handed system.

HMD is set in the coordinate system so that the mid-

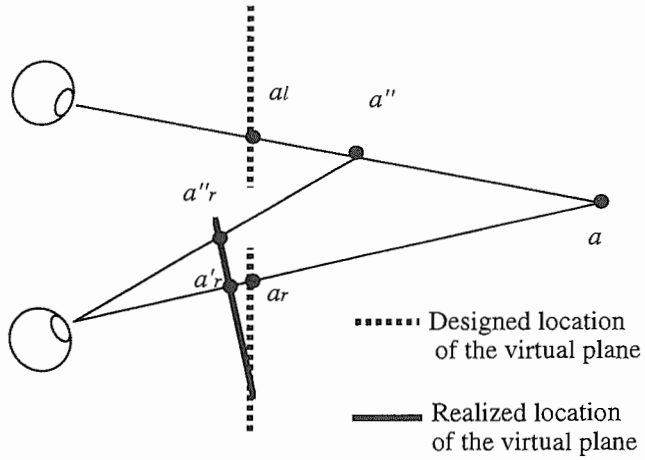

Figure 4. *Effect of mechanical misalignments.*

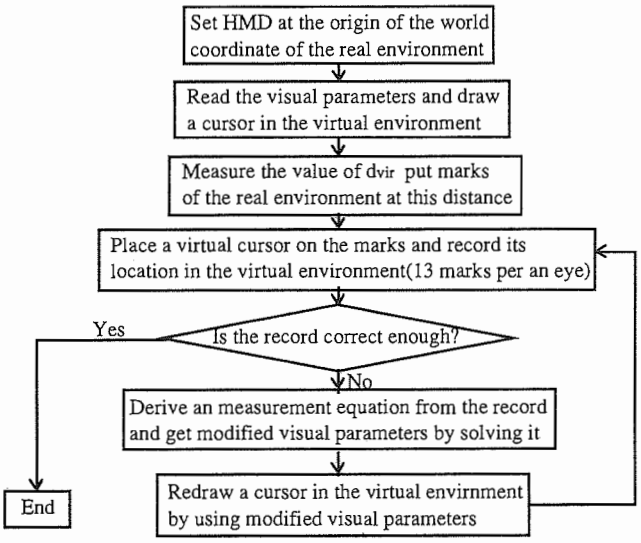

Figure 5. *Process of calibration.*

points of designed locations of the left and right eyes are at the origin and lines of sight are directed to the infinity point. The designed locations of the left and right eye are thus placed at (32.5, 0.0, 0.0) mm and (−32.5, 0.0, 0.0) mm in the coordinate system of the real environment, and the centers of designed locations of the virtual plane, the end point of the viewing vector, for the left and right eyes are (32.5, 0.0, 1000.0) mm and (−32.5, 0.0, 1000.0) mm.

As mentioned in Section 2.1, a plate P is installed on the HMD, and the designed locations of the eyes relative

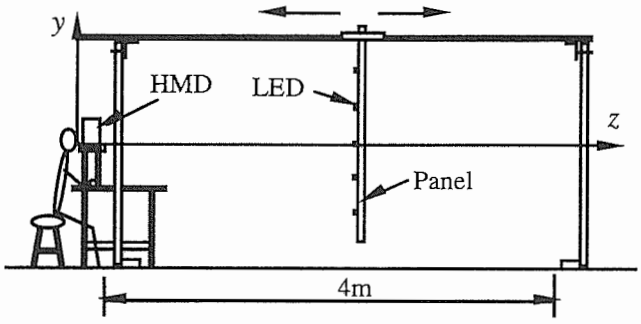

Figure 6. *Measurement system for calibration.*

to P are calculated based on drafts (Fig. 2b). Hence, what we actually have to do is measure the location of P in the coordinate system and to adjust it until the condition above is satisfied.

The panel, held by two rails, can move in the range 0.5 m $< z <$ 4 m. For convenience, the measurement is performed at 0.5, 1, 2, and 4 m.

3.1.2 Read Parameters of Projection Transformation and Draw a Cursor in the Virtual Environment. The virtual HMD is placed likewise in the virtual environment. The locations of the left and right eyes are thus (32.5, 0.0, 0.0) and (−32.5, 0.0, 0.0) in the coordinate system of the virtual environment, and the centers of the projection plane for the left and right eyes are (32.5, 0.0, 100.0) and (−32.5, 0.0, 100.0) since we have set l = 100 mm. The mark in the virtual environment is a cross-shaped cursor, which is movable by a joy stick.

3.1.3 Measure the Distance to Realized Virtual Plane (d'_{vir}) and Put Real Environment Markers at this Distance. As shown in Figure 6, a human operator directly controls the virtual cursor in a simulation of wearing the HMD. The effects of the two causes of error described in section 1 can coexist. The effects, however, can be eliminated by putting the panel at d'_{vir}, the distance to the center of the realized virtual plane, because this results in parallax only between the points on the virtual plane and on the panel. Conversely, it is possible to place the panel at d'_{vir} by using this phenomenon. Specifically, the operator swings his or her face up and down or left and right and observes the virtual cursor drawn

on the center of virtual plane while moving the panel back and forth until the movement parallax between the virtual cursor and the LED on the center of the panel disappears. The panel distance at which this occurs is d'_{vir}. Although the value of d'_{vir} is not directly the distance to the realized virtual plane, it is useful to derive this distance.

Once the STHMD coordinate system is set relative to the world coordinate system in step 3.1.1, the STHMD is firmly fixed at the calibration jig. Therefore, even if the operator moves his or her head a little, the STHMD does not move with it, only the relation between the actual and designed user's eye location changes. As a result, the operator is able to observe movement parallax between the virtual cursor and the panel LEDs.

3.1.4 Place a Virtual Cursor on the Marks and Record its Location Expressed in the Virtual Environment. Putting the panel at $z = d'_{vir}$, a human operator moves the virtual cursor so that it overlaps each LED, and records its location expressed in the coordinate system of the virtual environment. The records are used to calculate the shift of the virtual plane in step 3.1.5 and 3.1.6 if necessary. Although the HMD is originally a device for a binocular perception of the space, measurement for left and right eye can be done separately because the optical system for an eye is independent of the other. It is also desirable to avoid complex mutual interaction of the projection transformation parameters of both eyes.

3.1.5 Compare Recorded Locations with Original Locations Calculated According to the Designed Projection Transformation Parameters. If the recorded locations of the virtual cursor are accurate enough, we can exit from the calibration process according to the flowchart. The projection transformation parameters derived are used hereafter as calibration results. If the locations are not accurate enough, derive a measurement equation from the result of measurement and proceed to the next step. The measurement equation describes the relation between the result of measurement and errors of the projection transformation parameters. This equation is defined and solved in the subsequent steps to estimate the projection transformation parameters.

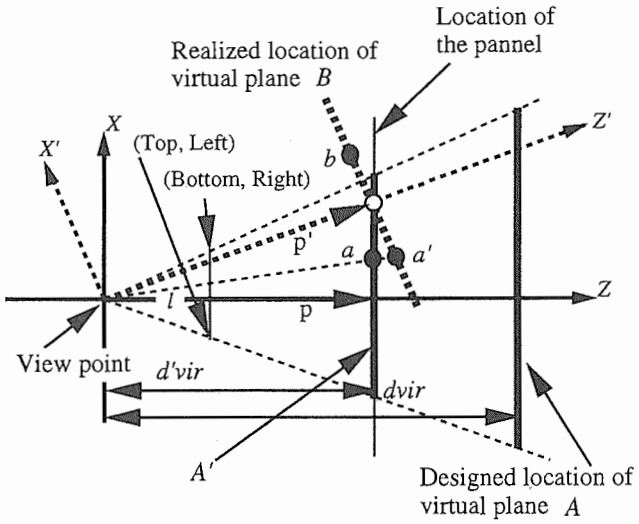

Figure 7. *Information obtained by the measurement.*

3.1.6 Derive a Measurement Equation. Consider the measurement result shown in Figure 7. The world coordinate system of the virtual environment $(O - x'y'z')$ seen through the HMD simultaneously exists on a world coordinate system of the real environment $(O - xyz)$ in the experiment system. The view point is the origin of both coordinate systems. Symbols used in the figure are

- A Designed virtual plane
- A' Substitute of designed virtual plane (LEDs are in this plane)
- B Realized virtual plane (expressed as a thick dotted line)
- $\mathbf{p}$ Designed line-of-sight vector
- $\mathbf{p}'_{vir}$ Temporary line-of-sight vector
- d_{vir} Distance to A
- d'_{vir} Distance to A' (center of B)
- l Distance to the projection plane

Before calibration, $\mathbf{p}'$, the temporary line of sight is in the direction of the center of the realized virtual plane "B" because, as shown in Figure 7, the location of "B" differs from that of designed virtual plane "A" and the difference is not reflected in the projection transforma-

tion parameters at this stage of calibration. The value of d'_{vir} was already determined in step 3.1.3, and the panel is located at this distance.

For convenience, we calculate the location of "B" relative to "A'," the substitute of "A" instead of comparing locations of "A" and "B," since there is no difference between locations of projection planes based on "A" and "A'." These are given by (*top, left*) and (*bottom, right*) in Figure 7. To calculate the location of "B," we may use "A" or "A'."

Suppose that there is an LED a on "A'" whose location expressed in $O - xyz$ is $\mathbf{a}_{\text{real}} = (a_x, a_y, d'_{\text{vir}})^T$. The virtual cursor whose location is considered to be equal to a is drawn at point b before the calibration. Point b expressed in the $O - x'y'z'$ coordinates is equal to a expressed in $O - xyz$, i.e., $\mathbf{b}_{\text{vir}} = (a_x, a_y, d'_{\text{vir}})^T$. The location of b relative to "B" is thus exactly the same as that of a relative to "A'."

Strictly, neither the length of $\mathbf{p}'$ nor the z component of $\mathbf{b}_{\text{vir}}$ is equal to d'_{vir}. However, we assume that the direction of $\mathbf{p}'$ does not differ from that of $\mathbf{p}$ very much, a few degrees at most, and that the length of $\mathbf{p}'$ may be considered equal to d'_{vir}. Besides, the effect of this assumption can be cancelled by taking it into account when we modify the size of the projection plane.

The measured location of the cursor, which is obtained by putting the cursor on an LED, is expressed as $\mathbf{a}'_{\text{vir}} = (a'_x, a'_y, d'_{\text{vir}})^T$ in $O - x'y'z'$. Since the difference between $\mathbf{a}_{\text{real}}$ and $\mathbf{b}_{\text{real}}$ is equal to the difference between "A'" and "B," we can calculate the location of "B" by using a matrix F, which maps $\mathbf{a}_{\text{real}}$ onto $\mathbf{b}_{\text{real}}$, on "A'" if F is known. As the value of $\mathbf{a}_{\text{real}}$ is already known, we need the value of $\mathbf{b}_{\text{real}}$ to calculate F. However, since the value of $\mathbf{b}_{\text{real}}$ is not measurable, we have to express F by known values, $\mathbf{a}_{\text{real}}$ and $\mathbf{b}_{\text{vir}}$, and measured value $\mathbf{a}'_{\text{vir}}$.

F is calculated from these values as follows. As mentioned before, the location of the projection plane is based on the location of the virtual plane. A thick line defined by (*top, left*) and (*bottom, right*) in Figure 8 represents the location of the projection plane based on "A'," which we defined in Figure 7. This is obtained by reducing "A'" by l/d'_{vir} in the direction of $\mathbf{p}$. The vector $\mathbf{p}$ indicates the designed line of sight. Its starting point is the view point, its end point is the center of "A'," and its

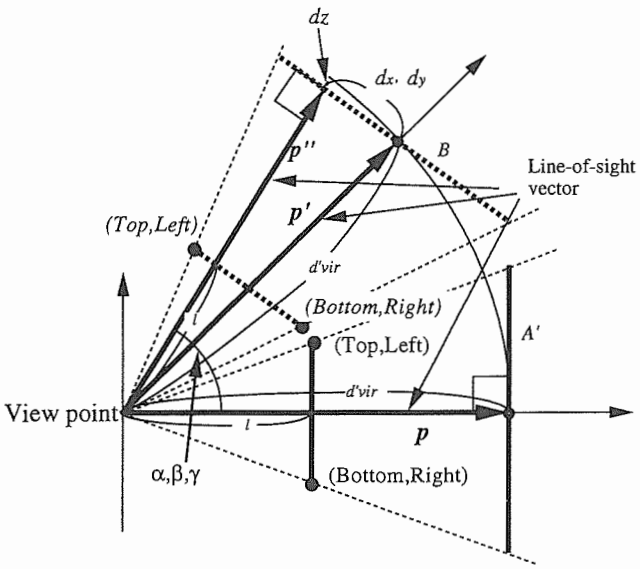

Figure 8. *Relation between the shift and rotation of virtual plane and parameters of projection transformation.*

length $\|\mathbf{p}\|$ is d'_{vir}. The realized virtual plane "B" is located differently from "A'." The projection plane based on "B" is given by (*top, left*) and (*bottom, right*). The vector $\mathbf{p}''$ indicates the correct line of sight and is perpendicular to "B." Its starting point is also the view point, but its end point is not necessarily the center of "B." The vector $\mathbf{p}'$, the temporary line of sight, is in the direction of the center of "B." The values of (*top, left*) and (*bottom, right*) are obtained by reducing "B" by $l/\|\mathbf{p}''\|$ in the direction of $\mathbf{p}''$ but we have to calculate $\|\mathbf{p}''\|$ during the calibration since it may differ from $\|\mathbf{p}'\| = d'_{\text{vir}}$.

The calibration method that we propose uses the following eight parameters to define a map F:

- Change the direction of the line-of-sight vector $\mathbf{p} \rightarrow \mathbf{p}'$ (described by ZYX Euler angles, α,β,γ),
- Shift the center of the projection plane from the viewing vector (d_x, d_y) and change the length of the viewing vector (d_z),
- Change the shape of the virtual planes (horizontal magnification a, vertical magnification b),

and calculate the location of "B." We then calculate the values of (*top, left*) and (*bottom, right*) by reducing "B" by $l/\|\mathbf{p}''\|$ in the direction of $\mathbf{p}''$.

Matrix R

$$R = \begin{pmatrix} c\alpha c\beta & c\alpha s\beta s\gamma - s\alpha c\gamma & c\alpha s\beta c\gamma + s\alpha s\gamma & 0 \\ s\alpha s\beta & s\alpha s\beta s\gamma + c\alpha c\gamma & s\alpha s\beta c\gamma - c\alpha s\gamma & 0 \\ -s\beta & c\beta s\gamma & c\beta c\gamma & 0 \\ 0 & 0 & 0 & 1 \end{pmatrix} \quad (5)$$

($s\alpha = \sin\alpha$, $c\alpha = \cos\alpha$ etc.) describes the change of the line-of-sight vector. The other parameters are compiled using matrix A

$$A = \begin{pmatrix} a & 0 & 0 & d_x \\ 0 & b & 0 & d_y \\ 0 & 0 & 1 & d_z \\ 0 & 0 & 0 & 1 \end{pmatrix} \quad (6)$$

These matrices describe a relation between $\mathbf{a}_{real}$ and $\mathbf{b}_{real}$ and the value of $\|\mathbf{p}''\|$ as follows:

$$\mathbf{b}_{real} = RA\mathbf{a}_{real} \quad (7)$$

$$\|\mathbf{p}''\| = d'_{vir} - d_z \quad (8)$$

The inverse transformation of (7) yields

$$\mathbf{a}_{real} = A^{-1}R^{-1}\mathbf{b}_{real} \quad (9)$$

which is equivalent to

$$\mathbf{a}_{vir} = A^{-1}R^{-1}\mathbf{b}_{vir} \quad (10)$$

because the mapping of $\mathbf{a}$ onto $\mathbf{b}$ is not affected by whether it is expressed in $O - xyz$ or $O - x'y'z'$. Since the z component of $\mathbf{a}'_{vir}$ is always d'_{vir}, and $\mathbf{a}'_{vir}$ and $\mathbf{a}_{vir}$ are in the same direction, we can express the relation between $\mathbf{a}'_{vir}$ and $\mathbf{a}_{vir}$ as

$$\mathbf{a}'_{vir} = \begin{pmatrix} \dfrac{d'_{vir}}{[\mathbf{a}_{vir}]_z} I & 0 \\ 0 & 1 \end{pmatrix} \mathbf{a}_{vir} \quad (11)$$

(I is a three-dimensioned unit matrix) where $[\mathbf{a}_{vir}]_z$ is the z component of $\mathbf{a}_{vir}$. With these results, the relation between the known value $\mathbf{b}_{vir}$ and observed value $\mathbf{a}'_{vir}$ is described as

$$\mathbf{a}'_{vir} = \begin{pmatrix} \dfrac{d'_{vir}}{[\mathbf{a}_{vir}]_z} I & 0 \\ 0 & 1 \end{pmatrix} A^{-1}R^{-1}\mathbf{b}_{vir} \quad (12)$$

By rewriting the right-hand portion of (12) as a function of the parameter vector $x = (a, b, \alpha, \beta, \gamma, d_x, d_y)$, we have

$$\mathbf{a}'_{vir} = \mathbf{h}(\mathbf{x}, \mathbf{b}_{vir})$$

$$= \begin{pmatrix} \dfrac{d'_{vir}\{a_x c\alpha c\beta + a_y s\alpha s\beta - d'_{vir} s\beta - d_x\}}{a\{a_x(c\alpha s\beta c\gamma + s\alpha s\gamma) + a_y(s\alpha s\beta c\gamma - c\alpha s\gamma) + d'_{vir} c\beta c\gamma - d_z\}} \\ \dfrac{d'_{vir}\{a_x(c\alpha s\beta s\gamma - s\alpha c\gamma) + a_y(s\alpha s\beta s\gamma + c\alpha c\gamma) + d'_{vir} c\beta s\gamma - d_y\}}{b\{a_x(c\alpha s\beta c\gamma + s\alpha s\gamma) + a_y(s\alpha s\beta c\gamma - c\alpha s\gamma) + d'_{vir} c\beta c\gamma - d_z\}} \\ d'_{vir} \end{pmatrix} \quad (13)$$

We then can calculate x by solving (13).

3.1.7 Estimation Using Modified Marquardt's Method.

We would like to modify the projection transformation parameters so that $\mathbf{a}'_{vir}$s are mapped onto $\mathbf{b}_{vir}$s with a minimum root mean square (RMS) error. This may be done using the least-squares method, a numerical solution that minimizes the error sum of squares with weight:

$$S = [\mathbf{a}'_{vir} - \mathbf{h}(\mathbf{x}, \mathbf{b}_{vir})]^T \Sigma^{-1} [\mathbf{a}'_{vir} - \mathbf{h}(\mathbf{x}, \mathbf{b}_{vir})]$$

$$\left(\sum_{ij} = \begin{cases} \sigma_i^2, & i = j \\ 0, & i \neq j \end{cases} \right) \quad (14)$$

In our measurement system, the maximum error in LED location is 3 mm, and this becomes the value of standard deviation σ. A nonlinear least square method is required to calculate $\mathbf{x}$ in our calibration method because $\mathbf{h}(\mathbf{x}, \mathbf{b}_{vir})$ is obviously a nonlinear model as (13) indicates. We selected the modified Marquardt's method in our procedure.

The Gauss–Newton method, the fundamental nonlinear least-squares method, modifies $\mathbf{x}$ repeatedly by

$$\mathbf{x}^{(k+1)} = \mathbf{x}^{(k)} + \Delta\mathbf{x} \quad (15)$$

where $\Delta\mathbf{x}$ is a modifier vector that is calculated as

$$(H^T \Sigma^{-1} H)\, \Delta\mathbf{x} = H^T \Sigma^{-1} \mathbf{v} \quad (16)$$

Equation (16) is called a normal equation and is derived from the measurement equation:

$$\mathbf{v} = \mathbf{a}'_{\text{vir}} - \mathbf{h}(\mathbf{x}, \mathbf{b}_{\text{vir}}) \tag{17}$$

and Jacobian matrix:

$$H_{ij} = \frac{\partial h_i}{\partial x_j} \tag{18}$$

By adding a diagonal matrix λI to (16), the modified Marquardt's method employs

$$(H^T \Sigma^{-1} H + \lambda I)\, \Delta\mathbf{x} = H^T \Sigma^{-1} \mathbf{v} \tag{19}$$

to calculate $\Delta\mathbf{x}$. The estimation starts with $\lambda = 0$, and the degree of nonlinearity is checked at every repetition. The λ increases when the degree of nonlinearity is large and decreases when it is small, which makes convergence of $\Delta\mathbf{x}$ more stable and rapid, and the whole calculation ends with the final value of λ being 0.

The values of the components of $\mathbf{x}$ are thus estimated, and the projection transformation parameters are recalculated based on them. In this way, we can eliminate the effect of mechanical misalignments.

3.1.8 Redraw the Virtual Environment and Return to Step 3.1.4. With modified parameters, redraw the virtual environment and reperform the measurement process of step 3.1.4.

3.2 Calibration of Differences between Actual and Designed Location of User's Eye on STHMD

3.2.1 Measurement of the Effect of Differences between Actual and Designed Location of User's Eye. As the result of the calibration above, points drawn in the virtual environment overlap real points through the whole space when the user's eyes are correctly located as designed. However, this is not always the case because the user's interocular distance and the shape of his or her face vary from one user to another.

Parallax errors appear between points in the real and virtual environment when the actual location of the user's eye differs from the designed location, because HMD projects all points on the virtual plane located at distance d_{vir} regardless of their actual distances. Figure 9 illustrates the effect of differences between actual and designed locations of the user's eye. Point a drawn in the virtual environment is projected onto the virtual planes for right and left eyes according to the designed locations of both eyes as a_l and a_r indicate. When the right eye, for example, is not located as designed and it is not reflected in the projection transformation parameters, a human operator feels that the point is drawn at a'' instead of a. If the projection transformation parameters are set according to the actual location of the right eye, the image of point a is supposed to be a'_r. We must therefore measure the actual locations of user's eyes and modify the projection transformation parameters according to the results.

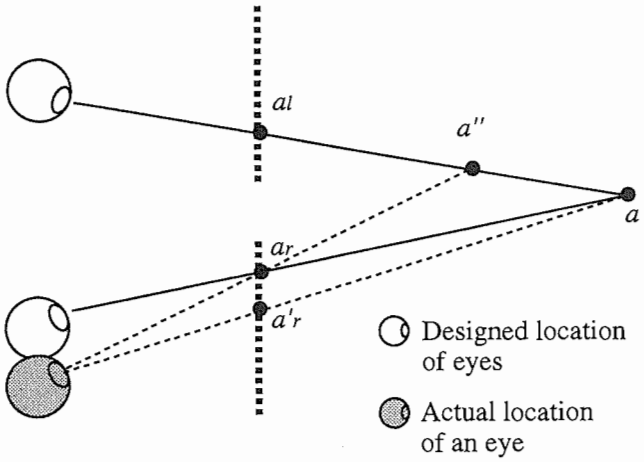

Figure 9. *Effect of differences between actual and designed location of user's eye.*

We cannot use the method mentioned in Section 3.1 in which the HMD is fixed at the origin of $O - xyz$ because this error should be calibrated during initialization every time a user starts using HMD. It is convenient that marks for the calibration are fixed at the HMD because the difference between the actual and designed eye location can be interpreted as a locational relation between the user's eye and HMD. This is why we put a removable plate P on the HMD as shown in Figure 2 and made it a basis for defining the designed locations of the user's eyes.

The original cause for parallax errors is the user's individual parameters mentioned above. However, consider-

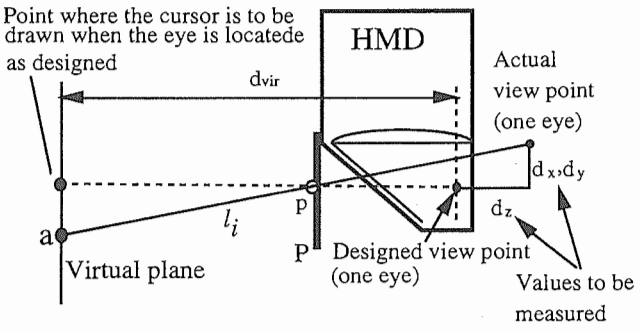

Figure 10. *HMD setup for calibration of eye's displacement.*

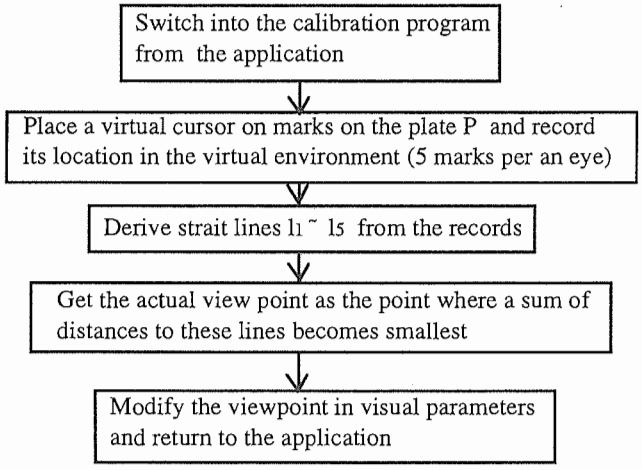

Figure 11. *Process of calibration of eye's displacement.*

ing that parallax error eventually appears as a shift of each eye from the designed location gives us a clearer idea. Therefore, we can discuss the calibration for one eye independently of that for the other. This can be done through the simple process below. Figure 10 shows an HMD setup for the calibration and Figure 11 shows the flowchart.

1. Switch from the application to the calibration process.
2. Place a virtual cursor on marks on the plate P and record its location expressed in the virtual environment (Fig. 10). Prepare five marks for each eye.
3. Derive straight lines $l_1 \sim l_5$ from the recorded values and the marks on P (Fig. 10).
4. Calculate the user's actual viewpoint (d_x, d_y, d_z) as the point that minimizes the sum of distances to straight lines $l_1 \sim l_5$.
5. Modify the viewpoint and return to the application.

3.2.2 Calculate the Actual Locations of User's Eyes. When the measured location of the virtual cursor is $\mathbf{a}_i = (a_i^0, a_i^1, d_{\text{vir}})$ and the corresponding mark on the plate P is $\mathbf{p}_i = (p_i^0, p_i^1, p_i^2)$, straight line l_i can be expressed as

$$l_i: \begin{pmatrix} x \\ y \\ z \end{pmatrix} = (\mathbf{a}_i - \mathbf{p}_i)t + \mathbf{p}_i = \begin{pmatrix} a_i^0 - p_i^0 \\ a_i^1 - p_i^1 \\ d_{\text{vir}} - p_i^2 \end{pmatrix} t + \begin{pmatrix} p_i^0 \\ p_i^1 \\ p_i^2 \end{pmatrix}. \quad (20)$$

$\mathbf{a}_i$ is a vector expressed in $O - x'y'z'$ and $\mathbf{p}_i$ is expressed in $O - xyz$. However, $\mathbf{a}_i$ and $\mathbf{p}_i$ can be directly used to calculate l_i as if they were expressed in the same coordinate system because $O - x'y'z'$ has precisely overlapped $O - xyz$ as a result of the calibration described in Section 3.1. The sum of distances from the point $\mathbf{d} = (d_x, d_y, d_z)$ to each straight line is

$$L = \sum_{i=1}^{5} \frac{|\mathbf{d} - \mathbf{p}_i|^2 |\mathbf{a}_i - \mathbf{p}_i|^2 - \{(\mathbf{d} - \mathbf{p}_i)(\mathbf{a}_i - \mathbf{p}_i)\}^2}{|\mathbf{a}_i - \mathbf{p}_i|^2}. \quad (21)$$

and the actual location of the user's eye is calculated as $\mathbf{d}$, which minimizes L. We can calculate the value of $\mathbf{d}$ by a linear least-squares method because (21) is a linear model.

Thus, the projection transformation parameters are modified based on $\mathbf{d}$. As a result, the STHMD can superimpose the virtual environment precisely on the real environment, wherever the realized virtual planes are located and wherever user's eyes are.

4 Experiment

In this section, we report the result of applying the proposed calibration method to the STHMD that we have made and show its effectiveness.

4.1 Elimination of Systematic Error Introduced in the Manufacturing Process

We set the STHMD at the origin of the world coordinate system of the real environment according to

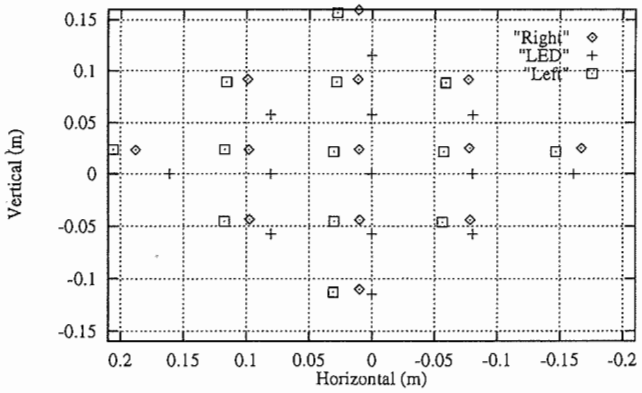

Figure 12. *Measured location of cursor at d_{vir} before calibration.*

step 3.1.1 of the process (Fig. 5) and measured d'_{vir} according to step 3.1.3. It was equal to 870 mm. We then put the panel at z = 870 mm to eliminate the effect of locations of observer's eyes at this stage of calibration and measured the values of $\mathbf{a}'_{vir}$ (locations of the virtual cursor which overlap LEDs on the panel).

Figure 12 shows the result of measurement. The horizontal and the vertical axes of Figure 12 represent the values of x and y on the panel. Although the locations were measured with the panel at z = 870 mm, we converted these values as if the panel were located at z = 1 m.

Because the HMD was set at the same location both in the real and the virtual environments, the virtual cursor should have correctly overlapped marks "+" that indicate locations of $\mathbf{b}_{vir}$ (i.e., $\mathbf{a}'_{vir}$, $\mathbf{b}_{vir}$, and $\mathbf{a}_{real}$ should have been equal if there were no difference between realized and designed locations of the virtual planes). Actually, however, we found that locations of $\mathbf{a}'_{vir}$ for both eyes were shown in Figure 12, exposing the shift of the virtual planes due to errors produced in the manufacturing process. Therefore, we had to go to step 3.1-6 to derive the measurement equation:

$$\mathbf{a}'_{vir} = \mathbf{h}(\mathbf{x}, \mathbf{b}_{vir}) \tag{22}$$

to estimate the shift of the realized virtual plane.

Table 2 summarizes how the projection transformation parameters were calibrated through the process mentioned above. Using the modified parameters, we reduced the errors expressed in Figure 12 as shown in Figure 13. Figure 14 shows the distribution of errors at each point "+" in Figure 13 (i.e., the difference between $\mathbf{b}_{vir}$ and $\mathbf{a}'_{vir}$). RMS errors for left and right eyes were 1.5 and 0.7 mm.

There was an error of 1 to 2 mm in the location of the drawn virtual cursor due to the low resolution of the LCDs. In addition, the experiment system also contains 3 mm errors (maximum) because this large system is hand-made, which directly produces errors in LED locations. The result of calibration is satisfactory under such a condition.

4.2 Eliminating of Errors Due to Location of User's Eye

As a result of the calibration above, points drawn in the virtual environment should have overlapped real points through the whole space when the user's eyes were correctly located as designed. However, we could not obtain such good results because locations of the observer's eyes differed from those designed. Figure 15 clearly shows the effect of parallax. One group of measurements at z = 0.5 mm had a tendency to shift to the left. However, groups measured at z = 1, 2, and 4 m had the opposite tendencies. These differences seem to depend upon whether z is less than d'_{vir} or not. Moreover, we clearly observed that the tendency to shift to the right increases as the differences between z and d'_{vir} increases.

Therefore, we also calibrated the effect according to the process of Figure 11. The result of estimating $\mathbf{d}$, which produces errors expressed in Figure 15, was (d_x, d_y, d_z) = (− 0.4, −0.7, −23.5 mm), and the errors were reduced as shown in Figure 16 by recalculating the projection transformation parameters based on the estimated value of $\mathbf{d}$. Table 3 compares RMS errors before and after the calibration. It was also satisfactory under the experimental conditions.

5 Future Works

Matching location and size of objects in the real environment with those in the virtual environment is

Table 2. *Projection Transformation Parameters Obtained by Calibration*

	Designed value	Actual value	
		Left eye	Right eye
d_{vir} (mm)	1000	854	869
Line of sight (mm)	(0, 0, 1000)	(13.4, 4.29, 870)	(−10.7, 5.72, 870)
Location of projection plane at z = 0.1 m (*right, bottom*) (mm)	(−36.0, −27.2)	(−38.6, −26.3)	(−32.9, −27.0)
Location of projection plane at z = 0.1 m (*left, top*) (mm)	(36.0, 27.0)	(28.4, 20.7)	(34.3, 20.2)

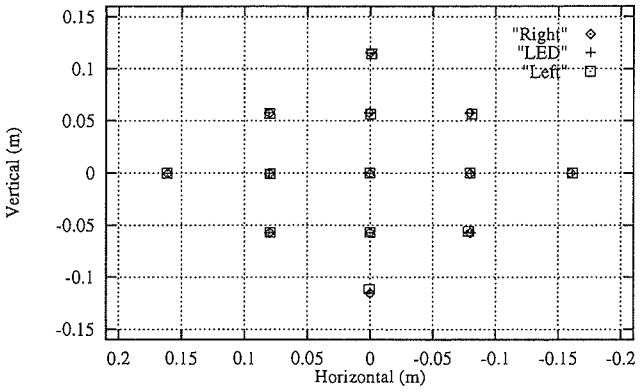

Figure 13. *Measured location of cursor at d_{vir} after calibration.*

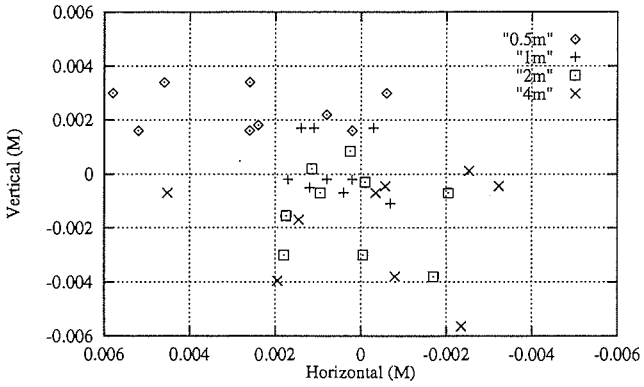

Figure 15. *Error caused by displacement of the eye (right eye).*

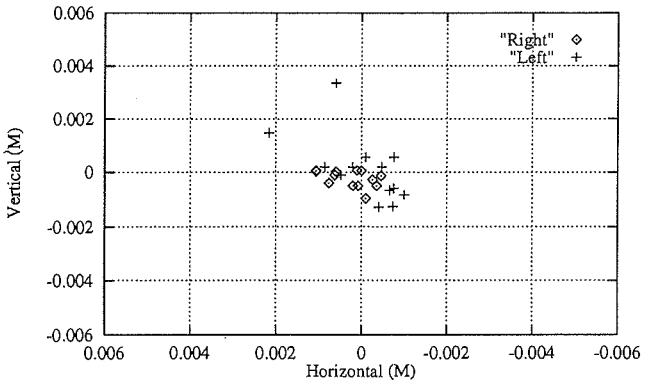

Figure 14. *Distribution of error at each point.*

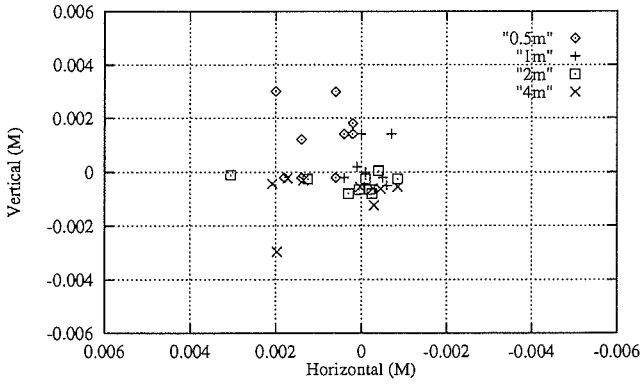

Figure 16. *Result of calibration of the eye's displacement.*

crucial for practical STHMD applications. In this paper, we have proposed a calibration method in which a precise correspondence between points in the real environment and the superimposed virtual cursor is obtained.

We divided the causes of errors into

- mechanical misalignments in STHMD, and
- differences between actual and designed location of user's eye on STHMD.

Table 3. *Comparison of RMS Error*

	0.5 m	1 m	2 m	4 m
Before calibration (mm)	4.2	1.5	2.4	3.6
After calibration (mm)	2.1	0.9	1.3	1.7

We then proposed methods to calibrate these error sources independently and demonstrated their effectiveness by executing them with our prototype.

However, this paper has not resolved the remaining error sources listed in Section 1. Resolving each error source is crucial for matching real and virtual environments. We must seek calibration methods to eliminate their effect and integrate them with our work presented in this paper to build a practically usable calibration procedure.

There may be more sophisticated methods to do the measurement in Section 3.1 than by using a human operator. It may also be necessary to try to view virtual objects other than panel LEDs to evaluate our method. These issues also require further discussion.

References

Azuma, R., & Bishop, G. (1994). Improving static and dynamic registration in an optical see-through HMD. *Proceedings of the SIGGRAPH '94,* 197–204.

Hirose, M., Kijima, R., Sato, Y., & Ishii, T. (1990). A study for modification of actual environment by see-through HMD. *6th Symposium on Human Interface,* Tokyo, 1–8.

Janin, A. L., Mizell, D. W., & Caudell, T. P. (1993). Calibration of head-mounted displays for augmented reality applications. *Proceedings of the IEEE Virtual Reality Annual International Symposium (VRAIS)*, 246–255.

Ma, J., Hollerbach, J. M., & Hunter, I. W. (1993). Optical design for a head-mounted display. *Presence: Teleoperators and Virtual Environments, 2*(3), 185–202.

McKenna, M., & Zeltzer, D. (1992). Three dimensional visual display systems for virtual environments. *Presence: Teleoperators and Virtual Environments, 1*(4), 45–62.

Robinett, W., & Rolland, J. P. (1992). A computational model for the stereoscopic optics of a head-mounted display. *Presence: Teleoperators and Virtual Environments, 1*(1), 45–62.

Tachi, S., & Arai, H. (1989). Design and evaluation of a visual display with a sensation of presence in tele-existence system. *Journal of the Robotics Society of Japan, 7*(4), 314–326.